Optical Engineering

OpticalEngineering.SPIEDigitalLibrary.org

Two-dimensional Fourier domain Ronchi ruling measurement using Talbot-based crossing point modeling

Sukmock Lee
Dae Wook Kim

SPIE.

Sukmock Lee, Dae Wook Kim, "Two-dimensional Fourier domain Ronchi ruling measurement using Talbot-based crossing point modeling," *Opt. Eng.* **59**(1), 014106 (2020), doi: 10.1117/1.OE.59.1.014106

Two-dimensional Fourier domain Ronchi ruling measurement using Talbot-based crossing point modeling

Sukmock Lee[a] **and Dae Wook Kim**[b,c,*]
[a]Inha University, Department of Physics, Incheon, Republic of Korea
[b]University of Arizona, Wyant College of Optical Sciences, Tucson, Arizona, United States
[c]University of Arizona, Steward Observatory, Tucson, Arizona, United States

Abstract. We propose a direct two-dimensional Fourier domain fitting-free method to determine the period of a Ronchi ruling. A precise method to measure a spatial frequency target's quality and fidelity is highly desired as the pattern period directly affects every aspect of a spatial frequency target-based metrology, including the accuracy and precision of the measurement or evaluations. A standard Talbot experimental apparatus and the Talbot effect are used to obtain and model our data. To determine the period of the ruling directly, only a common digital camera, with a protective glass and an air gap in front of the sensor array, and a Ronchi ruling of chrome deposited on a glass substrate are required. The Talbot effect-based crossing point modeling technique requires no calibration or *a priori* information but simply the pixel size of the digital camera and a precise means of measuring the spatial frequency from a Talbot image. For a Ronchi ruling with a period specification of 0.1 mm, the nanometric measurement was found to be 0.100010 mm with an error level of 5 nm. © *2020 Society of Photo-Optical Instrumentation Engineers (SPIE)* [DOI: 10.1117/1.OE.59.1.014106]

Keywords: Ronchi ruling; Talbot effect; Fourier analysis; period measurement.

Paper 191329 received Sep. 19, 2019; accepted for publication Dec. 18, 2019; published online Jan. 8, 2020.

1 Introduction

Ronchi rulings and many other periodic patterns are used for various vision and optical system calibration, metrology, and final performance evaluation applications. For instance, high-precision Ronchi ruling targets are often utilized for evaluating an imaging (or microscope) system's fine spatial resolution, parfocal stability performance, and field distortion quality. Also, the highly precise periodic test targets provide golden standard objects in order to evaluate and calibrate a microscopic imaging system's modulation transfer function performance or contrast imaging capability.

These spatial frequency pattern-based methods are one of the most straight forward and fundamental system-level optical performance check solutions. In industry, these targets are frequently used to test, maintain, troubleshoot, or cross-check various in-process optical systems, such as machine vision cameras and automatic inspection devices. By sliding a target along the optical axis, a system's depth of focus can also be measured. In the optical engineering community, many periodic targets and patterns have been widely used and well-accepted as a readily available standard component in technical memos, instrument manuals, academic publications, and so forth.

An objective and precise method to confirm (or measure) a spatial frequency target's quality and fidelity is highly desired and important. One of the fundamental characteristics of the ruling is the period, which directly affects every aspect of the spatial frequency target-based metrology including the accuracy and precision of the measurement or evaluations. Examples of the Ronchi test[1] and Talbot interferometry[2,3] are available in the literature. This study has developed a simple and practical method for determining the period of a Ronchi ruling. In particular, the most direct

*Address all correspondence to Dae Wook Kim, E-mail: letter2dwk@hotmail.com

and critical pioneering work utilizing Talbot effect for a high-precision metrology has been proposed using a numerically robust variogram-based approach by Herrera-Fernandez et al.[2] The method applied a variogram process to analyze realistic fringe data followed by a parametric fitting process. Utilization of the variogram is a powerful and practical approach since it enables a highly robust and accurate processing of actual data with strong noise suppression. Also, it is important to note that the proposed technique can be applied for measuring a collimation state or evaluating various beam characteristics, which sets a broader context of the applications.[4–6]

2 Talbot-Based Crossing Point Modeling

2.1 *Talbot Effect with a Periodic Ronchi Ruling*

The Talbot effect is the periodic appearance of self-imaging in a periodic structure, such as a ruling. This was first observed in 1836 by Talbot, and provides the foundation for the proposed method. For our purpose, the experimental apparatus consists of a point source of light, a positive lens, and a digital camera, in addition to the ruling to be measured. Despite the simplicity of the apparatus and the advantages of requiring no auxiliary optics, the proposed method requires no collimation calibrations or determination of the effective focal length of the lens.

If the ruling to sensor distance is zero, the period of any Talbot image is equal to the original value, independent of the collimation of the beam, but this requires a special camera with no protective glass, and placing the ruling directly on the sensor may damage the camera. For a typical digital camera, the sensor surface is protected by a glass window with some air gap.

Nonetheless, the combination of a protective window with some air gap, as in a typical digital camera, with a Ronchi ruling of chrome on a glass substrate is sufficient to determine the period of the ruling. No calibration is required as a prerequisite, no knowledge is required *a priori*, and no additional work is needed. Only the pixel size of the digital camera and a precise means of obtaining the spatial frequency from the Talbot image are required. For the latter, we adopt our recently developed method, the iterative local Fourier transform.[7] The remainder of this paper describes the theory behind the proposed method and presents the results of experiments to demonstrate its accuracy and efficacy.

Figure 1 shows a schematic layout of the experimental setup, where a Ronchi ruling of period p is illuminated by a converging beam following a positive lens and the diffracted field, called the Talbot image, is formed at the sensor plane (labeled as "camera" in Fig. 1), which is placed at distance d from the ruling. The intensity pattern in the image is measured by the sensor array in the camera. According to the geometrical optics, the Talbot image will be magnified by a factor of[3,8]

$$p' = p\left(1 - \frac{d}{z' - L_0}\right), \tag{1}$$

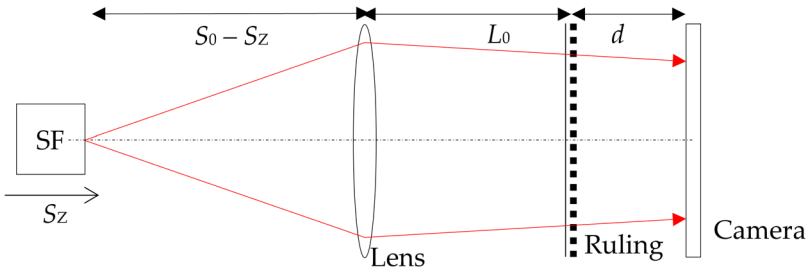

Fig. 1 Schematic diagram of the setup. The intensity pattern in the image is measured by the sensor array in the camera. SF is composed of a microscope objective and pinhole, d is the ruling-to-camera sensor distance, and L_0 is the lens-to-ruling distance. Here $S_0 - S_z$ is the object distance to the lens where S_0 is the unknown initial object distance and S_z is a micrometer reading of the SF translation.

where d is the ruling–camera sensor distance, L_0 is the lens–ruling distance, and z' is the radius of curvature for the converging beam wavefront after the lens. This radius of curvature corresponds to the image distance that can be computed from the conjugate image plane equation of a lens as[9]

$$\frac{1}{z}+\frac{1}{z'}=\frac{1}{f}, \tag{2}$$

where z is the object distance, or pinhole–lens distance, and f is the effective focal length of the lens. The self-imaging of Talbot effect corresponds to the case when the image distance becomes infinite with the object distance being equal to the effective focal length of the lens.

The translation stage on which the spatial filter (SF) is mounted allows a precise relative position change of the light source (i.e., object) from the lens using a micrometer attached to the stage. The object distance z can be expressed as

$$z = S_0 - S_z, \tag{3}$$

where S_z represents the readings from the micrometer (labeled in Fig. 1) and S_0 is the unknown initial object distance when $S_z = 0$.

By combining Eqs. (1)–(3), the period of the Talbot image can be expressed as

$$p' = p\left[1-\frac{d(S_o - S_z - f)}{(f-L_o)(S_o - S_z)+L_o f}\right]. \tag{4}$$

Equation (4) is general enough that it can also be used for a diverging beam and can be further approximated into a linear equation as

$$p' = a + bS_z, \tag{5}$$

where

$$\begin{cases} a = p\left[1-\frac{d(S_o-f)}{L_o f}\right] \\ b = \frac{pd}{L_0 f} \end{cases}, \tag{6}$$

when $f - L_0 \approx 0$. The approximation condition can easily be achieved by setting the lens–ruling distance to be approximately equal to the effective focal length of the lens.

2.2 *Crossing Point Modeling*

Figure 2 shows two simulated measures of the period of the ruling that correspond to two different values of the parameter d, whereas the others remain the same as computed using Eq. (4). When $d = 0$ or when the object distance is equal to the focal length of the lens, the period of the image will be equal to the original value, i.e., $p' = p$. Otherwise, the period varies monotonically with the value of S_z for the range shown in the figure. For the values used in the simulation, $S_z = 18.5$ mm corresponds to the case of collimation; the incident beam to the ruling is diverging when S_z is <18.5 mm and converging when S_z is >18.5 mm.

Note that it is impossible to distinguish whether the beam incident on the ruling is diverging or converging from a single set of measurements of the period, unless both the focal length of the lens and the point source to lens distance are known. The problem of distinguishing the collimation state of the incident beam makes the knowledge of the ruling period determinant.

However, the point of intersection of the two period measures given by two different values of d clearly indicates the value of the period. The two values of d expressed by the two slopes directly relate to the variation of the period via Eq. (4). Only when S_z is equal to the correct value for true collimation of the lens, do the periods in the measures using different d values become coincident. The unknown focal length does not affect the determination of the period, nor does the unknown exact point source to lens distance. This is the central point of the proposed method.

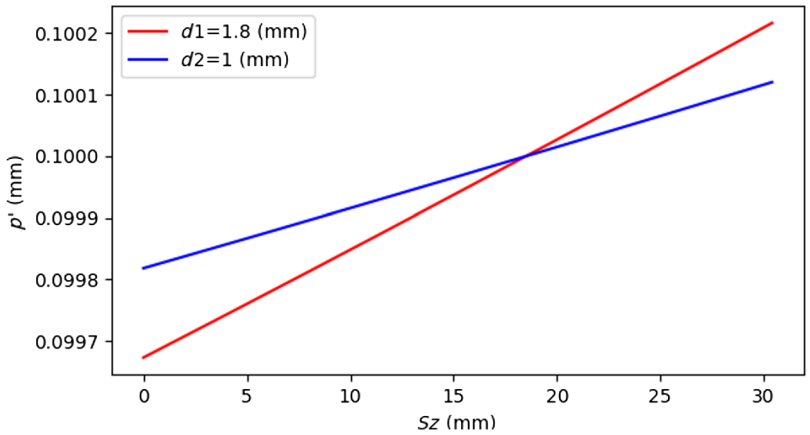

Fig. 2 Numerical simulated crossing periods as a function of S_z for two different values of d. Other parameters were fixed at $p = 0.1$, $f = 100$, $S_0 = 118.5$, and $L_0 = 90$ (mm). For the values used in the simulation, $S_z = 18.5$ mm corresponds to the case of collimation; the incident beam to the ruling is diverging when S_z is <18.5 mm, and converging when S_z is >18.5 mm.

3 Experimental Talbot Configuration and Data Acquisition Using Ronchi Ruling

3.1 *Integrated Talbot Configuration*

Figure 3 is a photograph of the actual setup. An SF with a pinhole of 5-μm diameter was used to make a point source of light ($\lambda = 532$ nm) diverging toward the lens. The circular beam of light from the lens was incident on a Ronchi ruling (Edmund Optics, duty cycle = 50%, period = 0.1 mm), and a monochrome CMOS board-level camera (Mightex Systems, MCN-B013, 1024×1280 pixels, 0.0052 μm per pixel) was used to acquire the Talbot images. The camera was connected to a PC through a USB cable and the images were saved for further analysis. The setup was the same as any typical Talbot effect apparatus but was positioned vertically with the camera facing up. The ruling was laid directly on the protective glass window of the camera after removing a lens mount.

The lens, ruling, and camera were all carefully aligned and fixed in position, and the laser and the SF were mounted on a translation stage that moved vertically with a micrometer. The reading

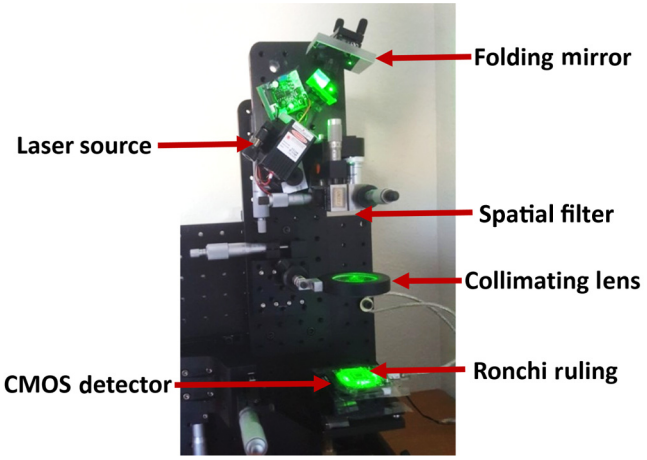

Fig. 3 Talbot effect-based experimental Ronchi ruling period measurement setup using a laser source. An SF with a pinhole of 5-μm diameter was used to make a point source of light ($\lambda = 532$ nm). The circular beam of light from the lens was incident on a Ronchi ruling, and a monochrome CMOS board-level camera was used to acquire the Talbot images.

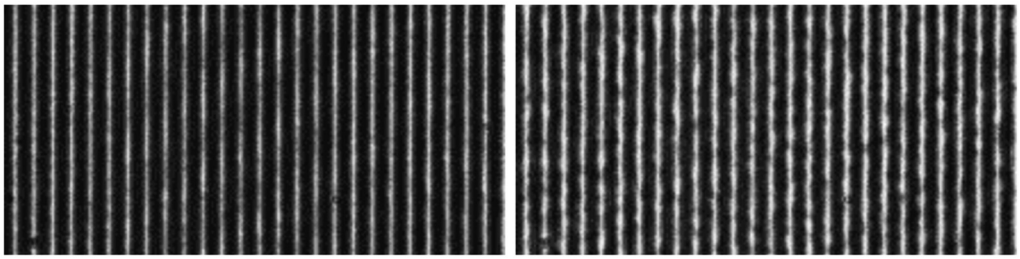

Fig. 4 Images measured at (a) $S_z = 12$ mm and (b) $S_z = 25$ mm. Each acquired Talbot image resembled the original ruling and was composed of dark and bright stripes. Both images exhibit 26 stripes but different duty cycles, and the number of stripes indicates a period of about 0.1024 mm.

of the micrometer, S_z, indicated the relative position of the pinhole with respect to the lens. The larger the value of S_z, the closer the pinhole was to the lens.

The lens used in the setup was selected from the lab stock, and the focal length of ~100 mm was a good fit to the apparatus. The pinhole–lens distance was adjusted so that the beam incident on the ruling would be collimated at around the middle of the micrometer travel. The existence of near-collimation was confirmed from the initial measurements. The measured value for the period of the acquired image was <0.1 mm at one end of the micrometer travel and >0.1 mm at the other end.

3.2 *Talbot Image Data Acquisition*

A set of measurements was then collected for the micrometer range $S_z = 12$ to 25 mm at increments of 0.5 mm. For $S_z = 12$ mm, the image point of the point source corresponded to a virtual image in which the beam beyond the lens was diverging, and the beam was converging with a real image for $S_z = 25$ mm. Each acquired Talbot image resembled the original ruling and was composed of dark and bright stripes, as shown in Fig. 4, where the two measured images at $S_z = 12$ and 25 mm have both been cropped to 256×512 pixels at the center of the images. Both images exhibit 26 stripes but different duty cycles, and the number of stripes indicates a period of about 0.1024 mm ($= 512 \times 0.0052/26$). Fast Fourier transform analysis of the images indicates that the period of the stripes is 0.0995 mm with a spectral peak at $(10.0473,0.0)$ mm^{-1} for $S_z = 12$ and 0.1005 mm with a spectral peak at $(9.9534,0.0)$ mm^{-1} for $S_z = 25$ mm.

The difference of 0.0939 mm^{-1} in the spectral peak (or 0.0010 mm in the period) between the two images is equivalent to just one spectral frequency interval for the fast Fourier transform analysis. A single spectral frequency interval for the 13-mm difference in position in S_z indicates either insufficient analysis for the period or a constant period within the inherent error level, a shortcoming of the fast Fourier transform.

4 Experimental Ronchi Ruling Measurement Result

4.1 *Iterative Local Fourier Transform Analysis*

To enhance the precision, we used the recently developed iterative local Fourier transform method,[8] which can achieve 210 times higher frequency resolution than the fast Fourier transform. Briefly, each image of 1024×1280 pixels was zero padded to create a 2048×2048 image, which fulfills the condition that the image array size is equal to a power of 2 for initial processing using the fast Fourier transform. The spectral peak was then identified and the frequency coordinate was narrowed down to find a better spectral peak of higher spectral intensity with 10 iterations of the iterative local Fourier transform as shown in Fig. 5. Each Talbot image (1024×1280 sampling) data processing took about 2 s using a computer with Intel® Core i7-8550U CPU and 8.00 GB memory.

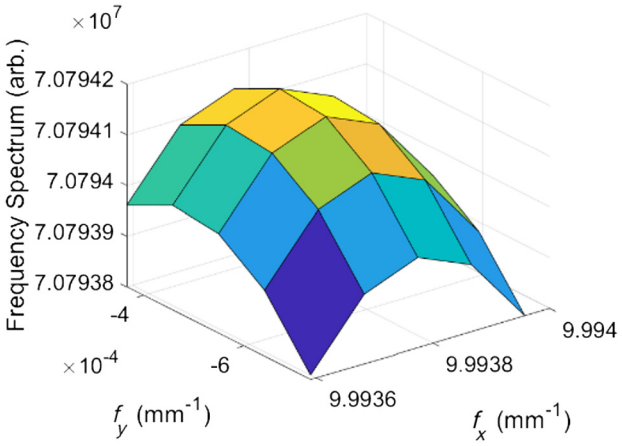

Fig. 5 The 2-D Fourier spectrum for the image shown in Fig. 4(b). The analyzed peak locates at $(9.9938, -0.0005)$ mm^{-1} and the corresponding period of the image is 0.100062 mm.

4.2 *Experiment Result of the Ronchi Ruling Measurement*

The 27 measured images were analyzed to determine their period, as shown in Fig. 6. The difference between the two images at $S_z = 12$ and 25 mm was now 0.000105 mm, around one-tenth of the 0.0010 mm obtained by the fast Fourier transform. The higher precision analysis also shows that the 27 periods are well separated and exhibit a linear trend, which clearly indicates that even small differences are not noise but real effects. The linear trend of the period values as a function of S_z indicates that the position of the pinhole could be varied even more finely if desired.

Unfortunately, Fig. 6 does not allow us to determine the precise period of the ruling, because the detected period changes with S_z. This problem, of which we were already aware,[10] is a result of the ruling not being in direct contact with the sensor surface due to the protective glass window. This small offset from ruling to sensor surface means the light rays forming the Talbot image continue to converge or diverge with changes in S_z as the rays propagate from ruling to sensor, and there is no way of knowing the true period of the ruling from this single set of measurements. However, it is obvious that the reason we cannot obtain the correct period is that there is a small but finite space between the ruling and the sensor surface. If there was a small change in this spacing, another set of measurements could be taken that would have a different slope from the first.

As expected from the theory, the two crossing linear trends in period (Fig. 7) clearly show that (1) the two trends in period coincide at $S_z = 18.5$ mm and (2) the periods between $S_z = 18$

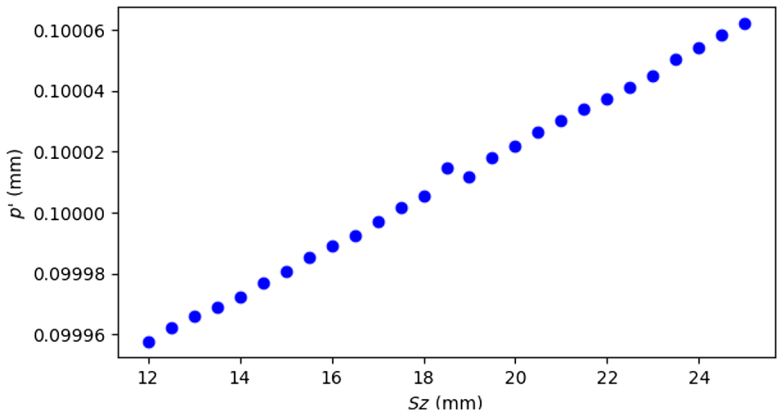

Fig. 6 Measured periods as a function of the pinhole location. The 27 measured images were analyzed to determine their period. The out-of-trend point near $S_z = 18.5$ mm is due to the ghost image effect, which provides another practical benefit of the presented linear fitting approach shown in Fig. 7.

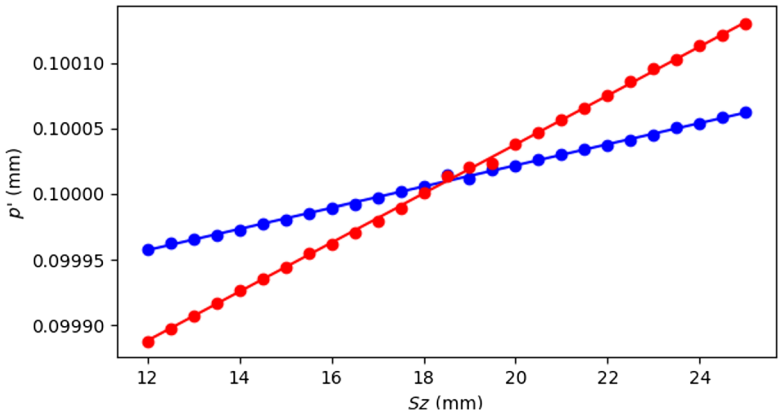

Fig. 7 Two sets of period measurements crossing at a critical point. To extract a better value, the periods were fitted to linear equations. The best-fit lines were $0.0000081S_z + 0.09986$ for the periods in blue and $0.0000187S_z + 0.09966$ for those in red. The two crossing linear trends in period clearly show that the two trends in period coincide at $S_z = 18.5$ mm and the periods between $S_z = 18$ and 19 mm are reversed as the theory predicts.

and 19 mm are reversed. These two facts imply that the actual period of the ruling is 0.10001 mm.

To extract a better value, the periods were fitted to linear equations. The best-fit lines were $0.0000081S_z + 0.09986$ for the periods in blue and $0.0000187S_z + 0.09966$ for those in red. These lines are also drawn in Fig. 7 and are clearly in good agreement with the corresponding data points. The intersection point computed from the best-fit lines confirms the measured value for the period of 0.100010 mm at $S_z = 18.5$ mm.

In taking the measurements, no calibration was involved and no assumptions were made, other than that the pixel size of the digital camera was as stated by the manufacturer. Although the Talbot effect and the scalar diffraction of light were employed, no computation regarding fundamental theories was needed. Only a set of computations for the precise spatial frequency was used to determine the precise period of the images.

We repeated the same measurements with different lens–camera distances (within 10 mm) and obtained an average value of 0.100010 mm with an error level of 5 nm. This observation justifies neglecting the slight variation in the lens to ruling distance produced by flipping the ruling. Thus, we conclude that the period of the ruling is 0.01% higher than the nominal value of 0.1 mm with an error level of 5 nm (0.005%). Our first attempts to determine the period of a linear grating such as a Ronchi ruling using the Talbot effect and a digital camera as a detector were foiled by the need to have a protective glass window in front of the camera sensor surface. We realized that, if two measurements were made with slightly different spacings between the camera sensor and ruling, we could precisely determine the ruling period by noting the position at which the two linear sets of data intersected on a graph of period versus the degree of collimation of the wavefront illuminating the ruling.

5 Concluding Remark

The iterative local Fourier transform-based solution is a direct two-dimensional (2-D) frequency-domain fitting-free approach. It directly investigates the frequency-domain information of the acquired raw fringe data without any filtering process using the enhanced Fourier transform solution. There are no fitting-associated error sources such as subjective (or physically unjustified) fitting parameter settings or data range trimming. Also, as a purely 2-D method unlike the other previously reported approaches (in Sec. 1), the accuracy of the frequency determination is fundamentally not affected by the clocking of the fringe image. While one may carefully set, check, adjust, and calibrate to minimize such clocking errors, which will alter the one-dimensional (1-D) profile's apparent frequency, it can be still one of the fundamental sources of an error. We also expect that the proposed direct 2-D Fourier domain approach can complement/

cross-check the 1-D variogram-based fitting solution[2] as an independent numerical data processing method.

Acknowledgments

We thank Robert Parks for his excellent comments on this paper. We also thank Luis Miguel Sánchez Brea and José María Herrera-Fernandez who shared their invaluable opinions and variogram-based computing codes.[2] Finally, this work was supported by Inha University, Incheon, Republic of Korea.

References

1. S. Lee and J. Sasian, "Ronchigram quantification via a non-complementary dark-space effect," *Opt. Express* **17**, 1854–1858 (2009).
2. J. M. Herrera-Fernandez et al., "Dual self-image technique for beam collimation," *J. Opt.* **18**, 075608 (2016).
3. L. M. Sanchez-Brea et al., "Self-imaging technique for beam collimation," *Opt. Lett.* **39**, 5764–5767 (2014).
4. R. Dubey and R. Kumar, "A simple setup for measurement of the coherence length of a laser diode using holographic optics," *Eur. J. Phys.* **40**, 055304 (2019).
5. S. Rana et al., "Automated collimation testing by determining the statistical correlation coefficient of Talbot self-images," *Appl. Opt.* **57**, 2686–2692 (2018).
6. J. Dhanotia, V. Bhatia, and S. Prakash, "Collimation testing using deflectometry in conjunction with windowed Fourier transform analysis," *Appl. Opt.* **56**, 2346–2352 (2017).
7. S. Lee, H. Choi, and D. W. Kim, "Precise and fast spatial-frequency analysis using the iterative local Fourier transform," *Opt. Express* **24**, 22110–22120 (2016).
8. J. Luo et al., "Long focal-length measurement using divergent beam and two gratings of different periods," *Opt. Express* **22**, 27921–27931 (2014).
9. R. Ditteon, *Modern Geometrical Optics*, Wiley, New York (1998).
10. Mightex Systems, private communication. No document is available online, but a detailed diagram of the camera can be provided on request.

Dae Wook Kim is an assistant professor of optical sciences and astronomy at the University of Arizona. His research area covers precision optical engineering, including interferometry and deflectometry. He is the chair of the Optical Manufacturing and Testing (SPIE) and Optical Fabrication and Testing (OSA) conferences. He is a senior member of OSA and SPIE and has served as an associate editor for the OSA *Optics Express* journal.

Biography of the other author is not available.